Supplementary Information: Ice dynamics and structural evolution of Jutulstraumen, Dronning Maud Land, East Antarctica (1963- 2022)

Table S1: Satellite images acquired during this study from 1963 to 2022 and associated error.

Date	Satellite	Resolution (m)	Co-registration error (m)	Mapping error (m)	Total error (m yr^{-1})
October,1963	ARGON	140			
18/11/1973	Landsat-1-Band 4	60	60	30	6
19/01/1985	Landsat-4-Band 4	30			
19/01/1985	Landsat-4-Band 4	30	30	15	12
08/10/1987	Landsat-4- Band 4	30			
08/10/1987	Landsat-4- Band 4	30	30	15	3
15/02/2000	Landsat-7-Band 8	15			
15/02/2000	Landsat-7-Band 8	15	15	7.5	9
02/12/2001	Landsat-7- Band 8	15			
02/12/2001	Landsat-7- Band 8	15	15	7.5	17
26/11/2002	Landsat-7- Band 8	15			
26/11/2002	Landsat-7- Band 8	15	15	7.5	4
02/02/2007	Landsat-7- Band 8	15			
02/02/2007	Landsat-7- Band 8	15	15	7.5	5
05/03/2010	Landsat-7- Band 8	15			
05/03/2010	Landsat-7- Band 8	15	15	7.5	17
01/03/2011	Landsat-7- Band 8	15			
01/03/2011	Landsat-7- Band 8	15	15	7.5	16
10/03/2012	Landsat-7- Band 8	15			
10/03/2012	Landsat-7- Band 8	15	15	7.5	18
18/02/2013	Landsat-8- Band 8	15			
18/02/2013	Landsat-8- Band 8	15	15	7.5	8
05/04/2015	Landsat-8- Band 8	15			
05/04/2015	Landsat-8- Band 8	15	15	7.5	19
19/02/2016	Landsat-8- Band 8	15			
19/02/2016	Landsat-8- Band 8	15	15	7.5	15
25/03/2017	Landsat-8- Band 8	15			
25/03/2017	Landsat-8- Band 8	15	15	7.5	9
06/03/2019	Landsat-8- Band 8	15			
06/03/2019	Landsat-8- Band 8	15	15	7.5	16
02/04/2020	Landsat-8- Band 8	15			

02/04/2020	Landsat-8- Band 8	15	15	7.5	11
05/10/2021	Landsat-8- Band 8	15			
05/10/2021	Landsat-8- Band 8	15	15	7.5	63
10/01/2022	Landsat-8- Band 8	15			

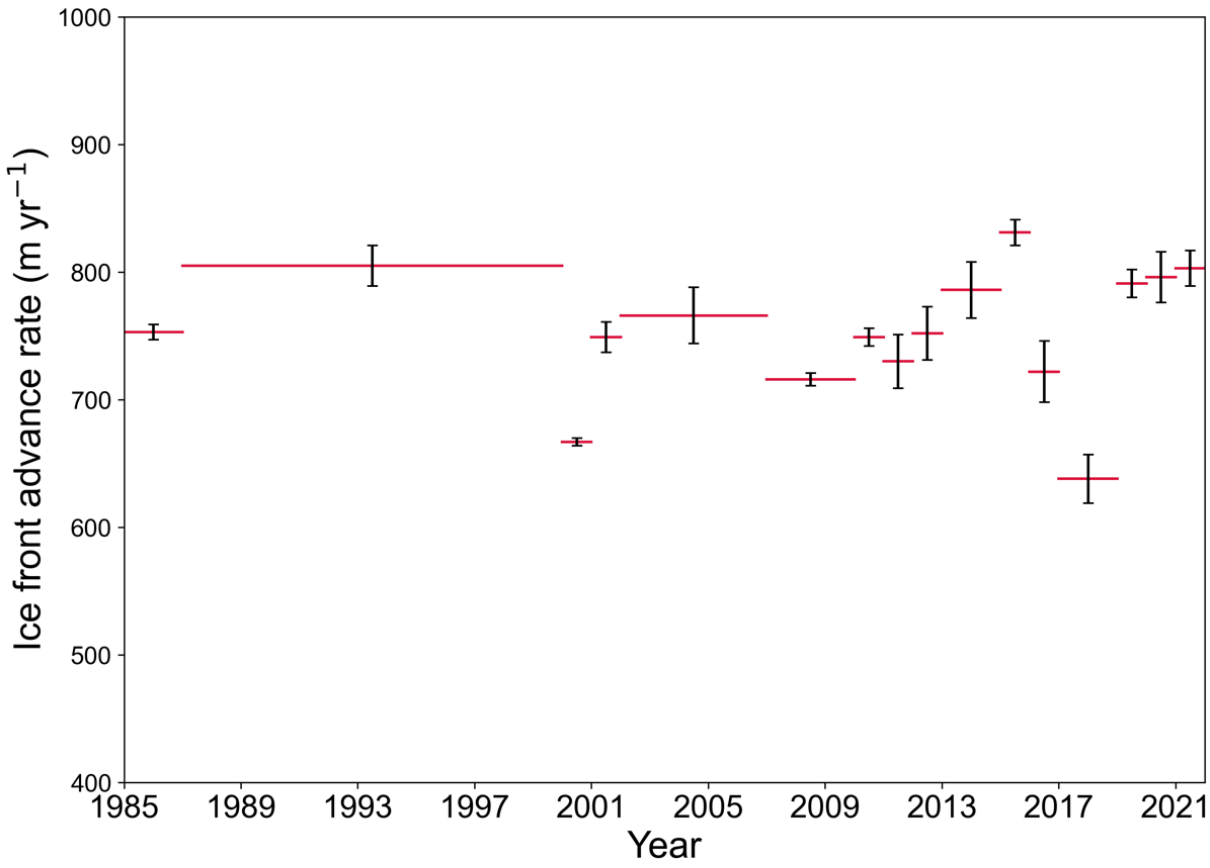

Fig. S1: Advance rate of main tongue of Jutulstraumen between 1985 and 2022. The red bars represent average advance rates over each period of measurement and black bars represent associated error (see supplementary Table S1).

Table S2: Percentage of velocity data coverage within each sampling box for Jutulstraumen. Missing values indicate that velocity data omitted from the analysis due to <20% data coverage or associated error is >50% of the mean velocity magnitude.

Year	Down-ice tongue	Up-ice tongue	Grounding line	Above GL
2000	-	30	47	22
2002	-	80	64	21
2003	-	31	-	-
2006	-	-	-	-
2007	22	65	64	59

2008		76	66	83
2009		86	59	28
2010	59	98	70	51
2011		88	63	24
2012	-	26	-	-
2013	85	100	100	100
2014	100	100	100	100
2015	100	100	100	100
2016	100	100	100	100
2017	100	100	100	100
2018	100	100	100	100

Table S3: The average rate of thinning and thickening of grounded ice observed at four locations inland of the grounding line of Jutulstraumen between 2003 and 2020 using dataset provided by Schröder et al. (2019), Nilsson et al. (2022) and Smith et al. (2020)

Distance from grounding line (upstream) (km)	**Schröder et al. (2019) (2003-2017) (m yr^{-1})**	**Nilsson et al. (2022) (2003-2020) (m yr^{-1})**	**Smith et al. (2020) (2003-2019) (m yr^{-1})**
20	+0.14 ± 0.1	+0.18 ± 0.04	+0.15±0.004
60	+0.11 ± 0.1	+0.1 ± 0.03	+0.19±0.006
80	+0.1 ± 0.1	+0.17 ± 0.04	+0.14±0.003
120	+0.07 ± 0.01	+0.11 ± 0.02	+0.17±0.001

Table S4: Propagation rates and 95% confidence intervals (m d^{-1}) derived from measured rift lengths of western margin of Jutulstraumen using MODIS imagery

SEASON	RW1	CI	RW2	CI	RW3	CI	RW4	CI	RW5	CI	RW6	CI	RW7	CI
CASE A														
2003/04	8.4	2.2	5.7	2.3	23.1	10.9	2.1	0.3						
2004/05	4.4	1.3	7.2	3.1	13.5	6.3	3.6	2.3						
2005/06	2.2	0.7	-1.4	0.7	0.4	0.3	0.2	1.8	5.8	3.1				
2006/07	4.8	1.3	0.4	0.2	3.3	0.1	4.2	0.1	14.9	8.4				
2007/08	14.4	9.4	-4.4	1.2	-0.9	0.3	4.7	0.3	5.1	1.3				
2008/09	0.9	0.2	-1.2	0.2	1.4	0.5	51.1	12.1	-2.8	0.5				
2009/10			33.9	12.2	24.7	9.6	16.5	5.6						
2010/11	15.2	7.1	-4.8	0.8	6.8	2.4	35.5	23.2	27.1	3.3	12.5	9.3		
2011/12	2.2	0.4	-0.2	0.1							-0.1	0.4		
2012/13	-3.1	1.2	-6.1	1.3							-4.8	0.1		
2013/14	-3.1	1.3	1.4	0.06							-2.1	0.1		
2014/15	0.07	0.1	-3.7	0.2							0.4	0.2		
2015/16														
2016/17	1.5	0.2	-1.4	0.2							0.04	0.02	3.8	0.3
2017/18														
2018/19	7.3	2.5	-0.1	0.2							0.9	0.04	8.4	6.7
2019/20	2.2	0.3	-6.5	1.1							20.6	17.1	-0.3	4.3
2020/21			-3.3	0.2							0.5	0.6		
2021/22	3.9	0.2	-0.7	0.6							1.0	0.06	3.6	0.4
CASE B	0.2	0.1	0.4	0.3	0.2	0.02	0.5	0.2	0.4	0.04	0.3	0.08	0.1	0.07
CASE C	1.5	0.1	0.2	0.06	1.9	0.4	8	1.1	1.6	0.4	1.5	0.2	1.6	0.3

Table S5: Propagation rates and 95% confidence intervals (m d^{-1}) derived from measured rift lengths of Eastern margin of Jutulstraumen using MODIS imagery.

SEASON	RE1	CI	RE2	CI	RE3	CI	RE4	CI	RE3+RE4	CI	RE5	CI	RE6	CI	RE7	CI	RE8	CI
CASE A																		
2003/04	2.9	0.1	3.2	0.2	-1.4	0.2	2.4	1.3			5.8	3.6	13.1	4.7	1.0	0.5		
2004/05	-1.2	0.1	3.6	3.0	-1.5	0.01	2.6	1.0			-4.4	1.2	0.9	0.4	-0.3	0.1		
2005/06	-0.4	0.2	-10.9	4.3	-3.8	3.1	-2.0	0.1			-1.4	0.3	2.4	0.9	4.2	2.1		
2006/07	1.5	0.5	2.5	0.5	-4.4	2.4	6.4	0.4			5.6	2.2						
2007/08	1.3	0.3	-10.5	8.7	-3.4	0.2	6.8	2.5			-0.4	0.2						
2008/09	-1.9	0.2	0.5	0.3	10.5	5.3	1.3	0.4			-3.4	0.2						
2009/10	6.6	0.5									5.6	2.5						
2010/11	1.2	2.0	-0.7	0.1							6.7	3.3						
2011/12		0.1		0.1								6.1						
	0.1		-1.5						1.7	1.0	9.5							
2012/13	-2.9	0.2	-2.0	0.2					4.2	2.4	4.7	2.7						
2013/14	1.0	0.5	-3.7	0.1					5.2	2.1	-1.2	0.6					6.4	2.2
2014/15	0.6	0.2	-6.3	0.2					5.5	0.6	2.5	0.6						
2015/16																		
2016/17		0.1		1.1						0.5		0.4						10.5
	-1.3		8.8						-2.0		1.7						27.4	
2017/18																		
2018/19	4.3	0.1	1.2	0.2					2.9	0.2	5.7	2.4					7.7	3.5
2019/20		0.2		1.3								10.3						15.3
	-0.3		1.5						10.7	5.8	22.4						29.9	
2020/21	3.5	0.2	3.3	0.2							1.5	0.6						

2021/22	1.7	1.2	-1.7	1.1					2.5	0.2	11.2	5.2				0.8		0.2
CASE B	0.1	0.04	0.1	0.05	0.4	0.3	0.8	0.3	0.4	0.2	0.2	0.1	2.1	0.5	1.2.	0.8	0.04	0.01
CASE C	0.1	0.03	0.1	0.08	0.1	0.1	0.6	0.3	0.3	0.06	0.7	0.07	1.4	0.9	0.1	0.08	3.2	0.4

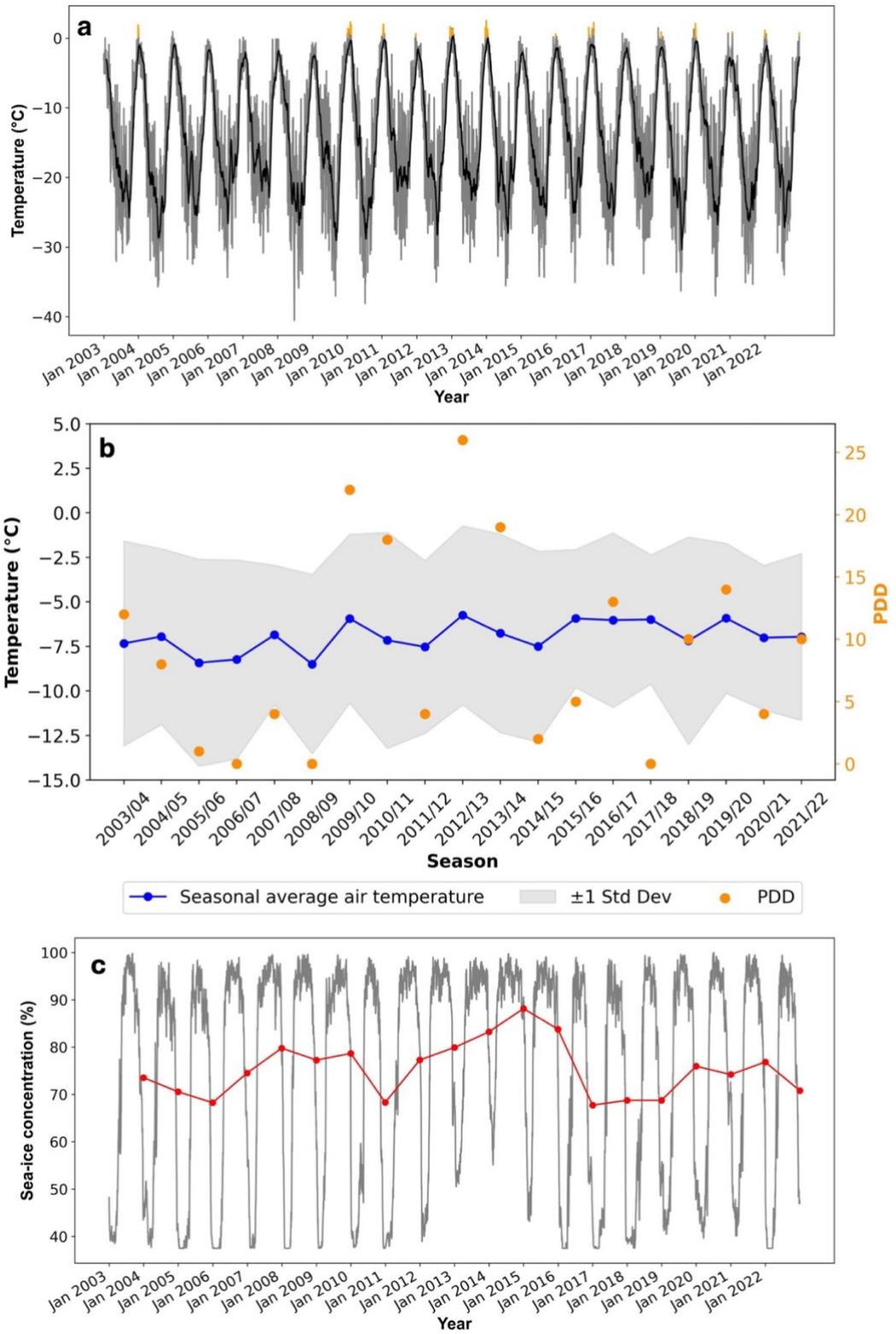

Fig. S2: (a) Daily averaged 2 m air temperature in grey overlaid with 6-month moving average (in black) and orange highlights denotes temperature > 0ºC. (b) Average austral summer air temperatures over Jutulstraumen from 2003 to 2022 (blue). The shaded region indicates the 1 standard deviation (grey), while the orange markers represent the number of PDDs for each austral summer. (c) daily averaged sea-ice concentration in grey overlaid with summer average sea-ice concentration (%) (red).

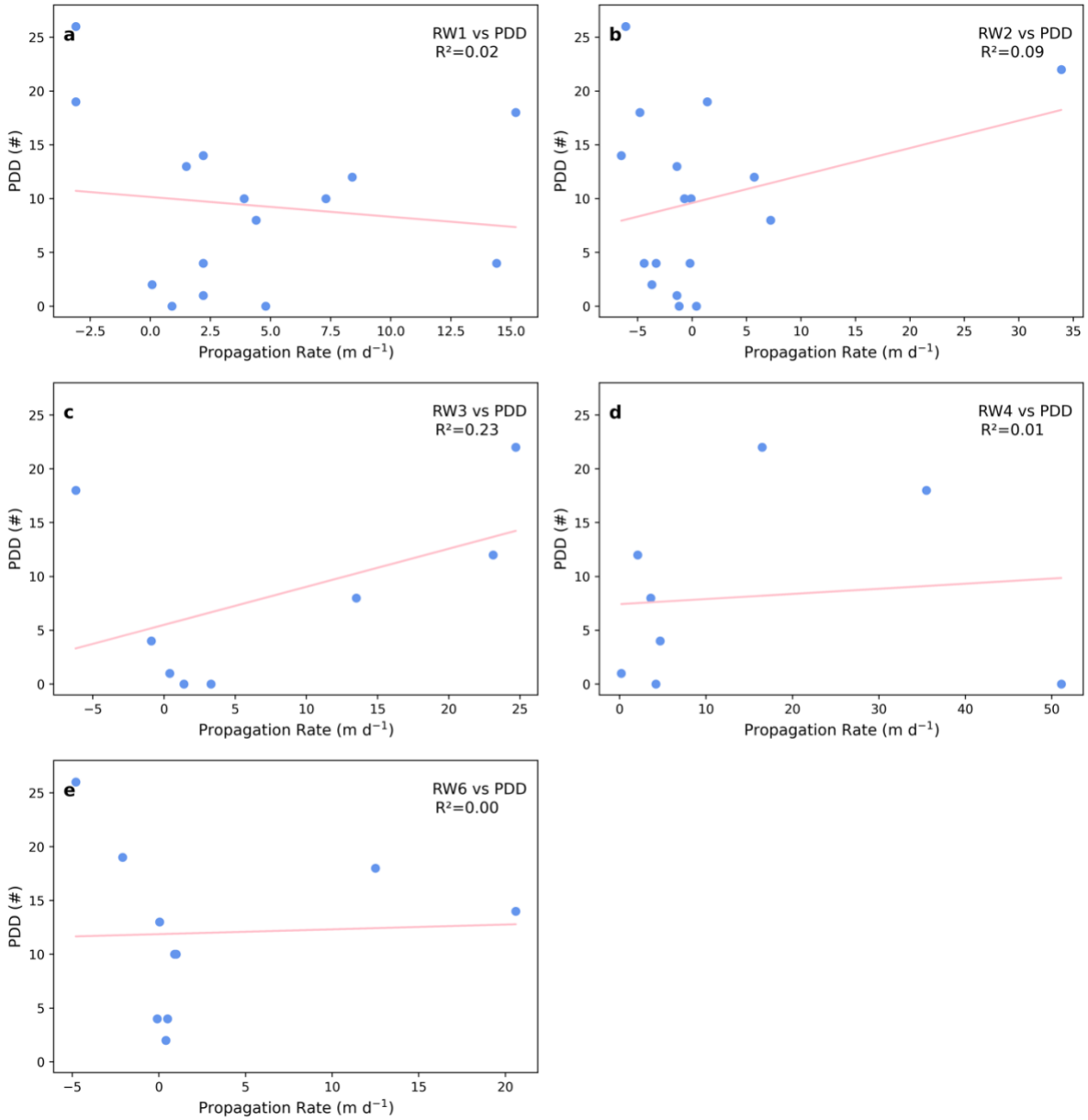

Fig. S3: Scatter plots illustrating the relationship between propagation rates of rifts on the western margin (RW) and positive degree days (PDD). Subplots (a) through (f) correspond to RW1, RW2, RW3, RW4, RW5, RW6 and RW7, respectively. Each subplot presents a fitted linear regression line to highlight the correlation between the propagation rate and PDD for each rift. RW5 and RW7 were omitted from the figure because each has fewer than five data points, and such small sample sizes can yield unreliable estimates.

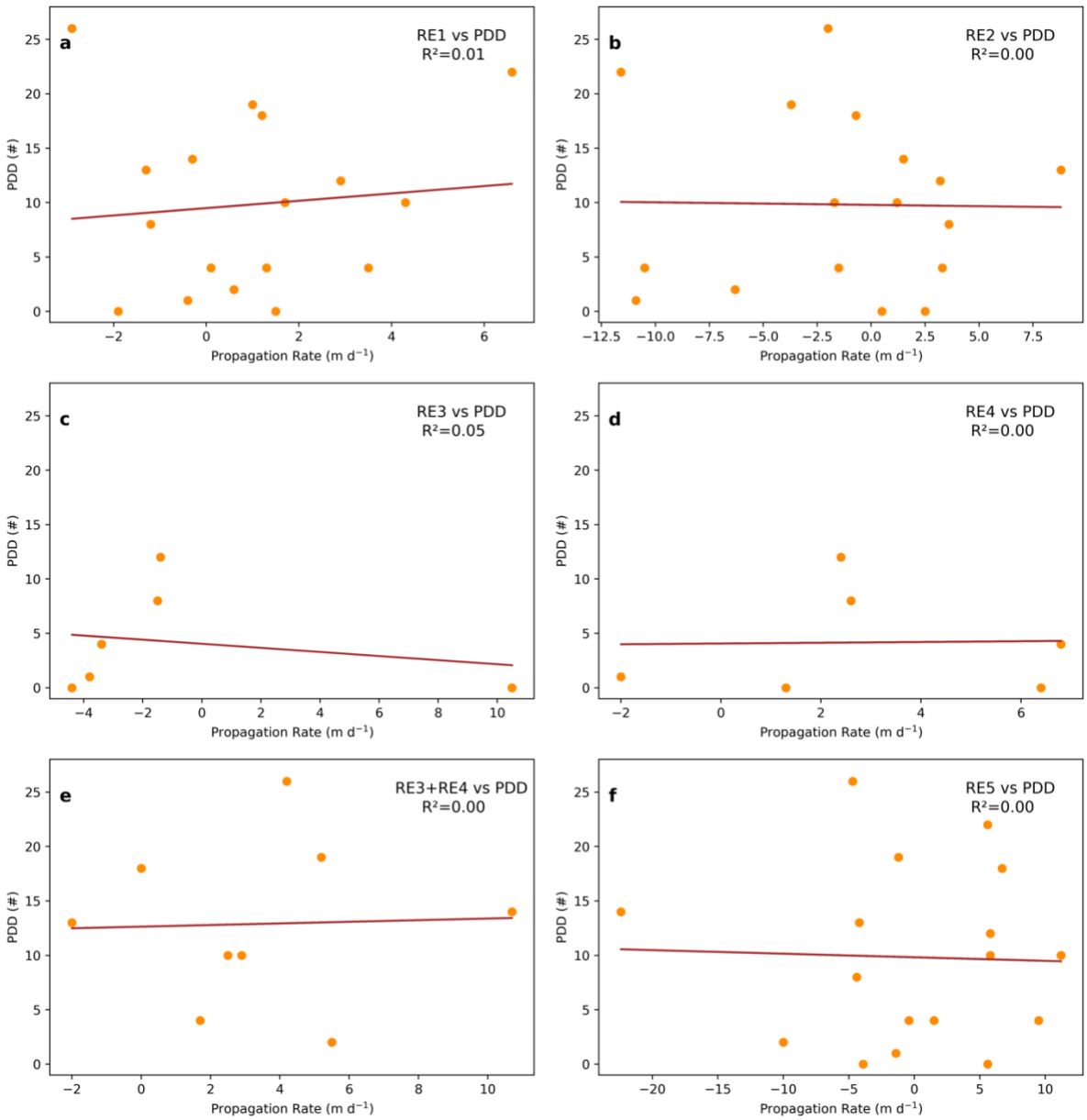

Fig. S4: Scatter plots illustrating the relationship between propagation rates of rifts on the eastern margin (RE) and positive degree days (PDD). Subplots (a) through (f) correspond to RE1, RE2, RE3, RE4, RE5, and RE8, respectively. Each subplot presents a fitted linear regression line to highlight the correlation between the propagation rate and PDD for each rift. We only consider the correlation coefficients for rifts that have been present for more than three summer seasons; hence, RE6, RE7 and RE8 are not included due to the limited data (less than 5 data points), which would render the correlation coefficients less reliable.

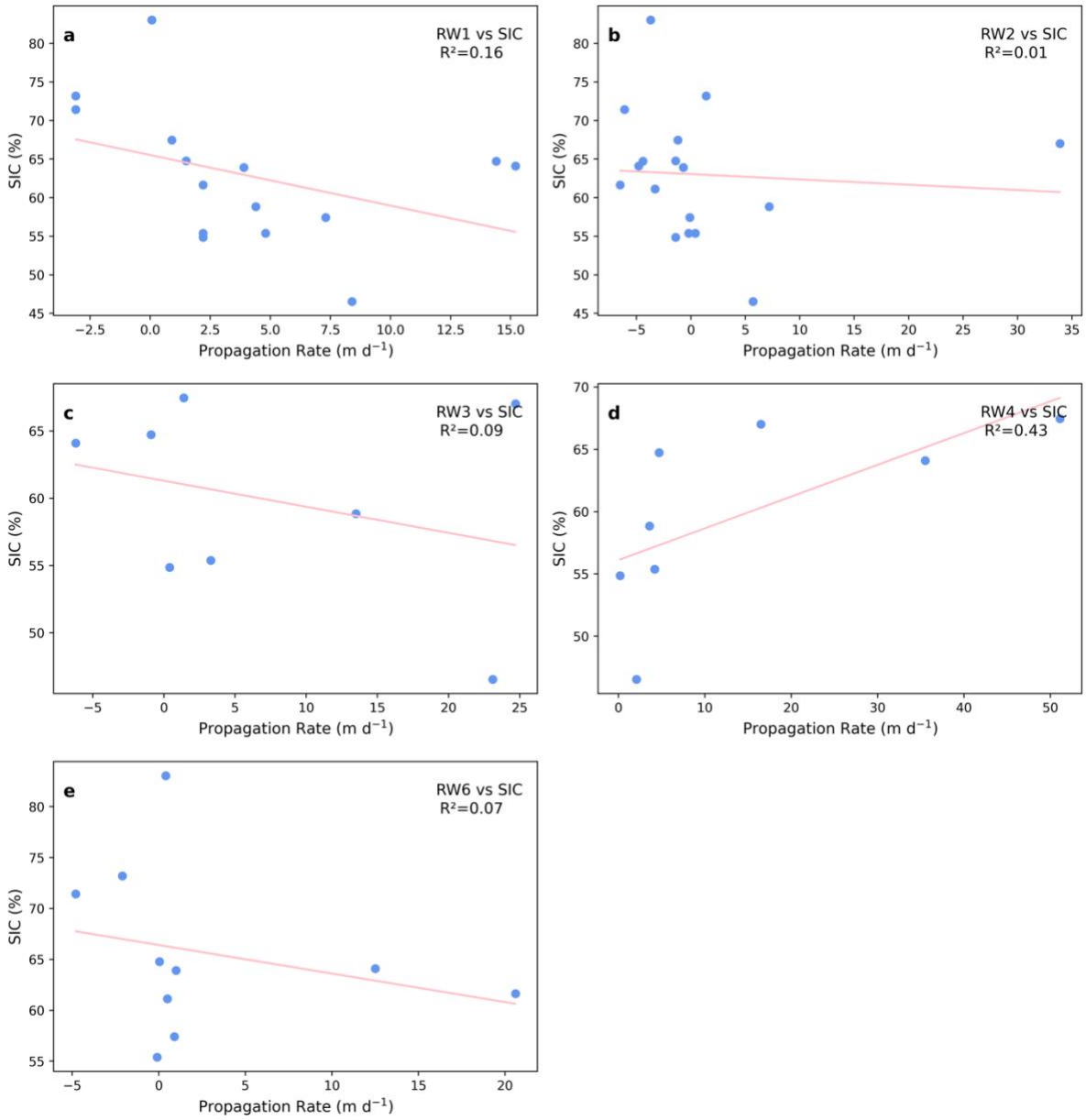

Fig. S5: Scatter plots illustrating the relationship between propagation rates of rifts on the western margin (RW) and summer mean sea ice concentration (%). Subplots (a) through (f) correspond to RW1, RW2, RW3, RW4, RW5, RW6 and RW7, respectively. Each subplot presents a fitted linear regression line to highlight the correlation between the propagation rate and summer mean sea ice concentration (%) for each rift. RW5 and RW7 were omitted from the figure because each has fewer than five data points, and such small sample sizes can yield unreliable estimates.

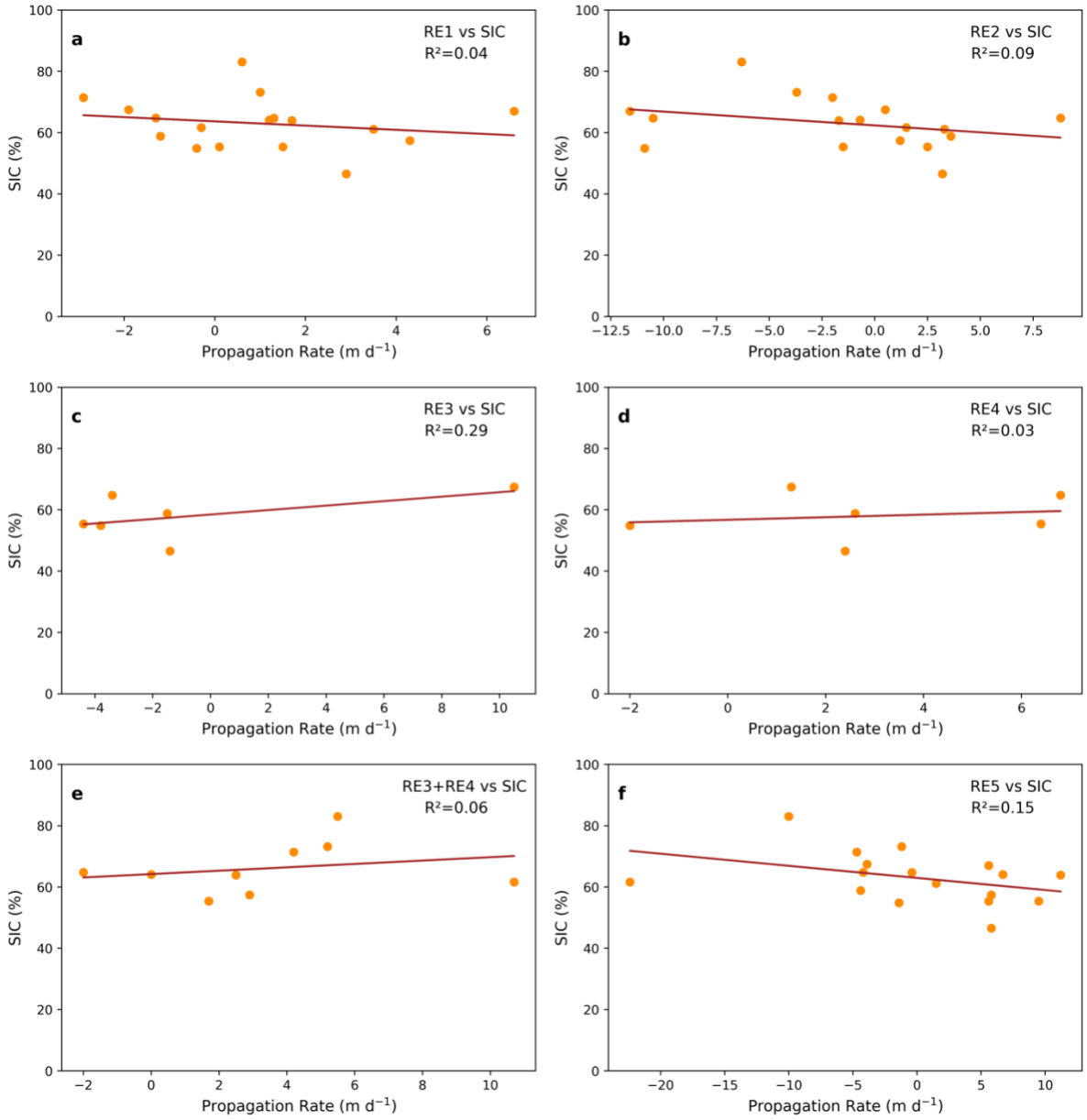

Fig. S6: Scatter plots illustrating the relationship between propagation rates of rifts on the eastern margin (RE) and summer mean sea ice concentration (%). Subplots (a) through (f) correspond to RE1, RE2, RE3, RE4, RE5, and RE8, respectively. Each subplot presents a fitted linear regression line to highlight the correlation between the propagation rate and summer mean sea ice concentration (%) for each rift. We only consider the correlation coefficients for rifts that have been present for more than three summer seasons; hence, RE6, RE7 and RE8 are not included due to the limited data (less than 5 data points), which would render the correlation coefficients less reliable.